The Astrophysical Journal Letters, 807:L9 (5pp), 2015 July 1 doi:10.1088/2041-8205/807/1/L9

AN ULTRA-LUMINOUS QUASAR AT $z = 5.363$ WITH A TEN BILLION SOLAR MASS BLACK HOLE AND A METAL-RICH DLA AT $z \sim 5$

Feige Wang[1,2], Xue-Bing Wu[1,3], Xiaohui Fan[2,3], Jinyi Yang[1,2], Zheng Cai[2], Weimin Yi[4,5], Wenwen Zuo[6], Ran Wang[3], Ian D. McGreer[2], Luis C. Ho[1,3], Minjin Kim[7], Qian Yang[1], Fuyan Bian[8,9], and Linhua Jiang[3]

[1] Department of Astronomy, School of Physics, Peking University, Beijing 100871, China; feige.wang@pku.edu.cn
[2] Steward Observatory, University of Arizona, 933 North Cherry Avenue, Tucson, AZ 85721, USA
[3] Kavli Institute for Astronomy and Astrophysics, Peking University, Beijing 100871, China
[4] Yunnan Observatories, Chinese Academy of Sciences, Kunming 650011, China
[5] Key Laboratory for the Structure and Evolution of Celestial Objects, Chinese Academy of Sciences, Kunming 650011, China
[6] Shanghai Astronomical Observatory, Chinese Academy of Sciences, Shanghai 200030, China
[7] Korea Astronomy and Space Science Institute, Daejeon 305-348, Korea
[8] Mount Stromlo Observatory, Research School of Astronomy and Astrophysics, Australian National University, Weston Creek, ACT 2611, Australia

Received 2015 April 7; accepted 2015 June 4; published 2015 June 26

ABSTRACT

We report the discovery of an ultra-luminous quasar J030642.51+185315.8 (hereafter J0306+1853) at redshift 5.363, which hosts a supermassive black hole with $M_{\rm BH} = (1.07 \pm 0.27) \times 10^{10}\,M_{\odot}$. With an absolute magnitude $M_{1450} = -28.92$ and a bolometric luminosity $L_{\rm bol} \sim 3.4 \times 10^{14} L_{\odot}$, J0306+1853 is one of the most luminous objects in the early universe. It is not likely to be a beamed source based on its small flux variability, low radio loudness, and normal broad emission lines. In addition, a $z = 4.986$ damped Lyα system (DLA) with $[{\rm M/H}] = -1.3 \pm 0.1$, among the most metal-rich DLAs at $z \gtrsim 5$, is detected in the absorption spectrum of this quasar. This ultra-luminous quasar puts strong constraints on the bright end of the quasar luminosity function and massive end of the black hole mass function. It will provide a unique laboratory for the study of BH growth and the co-evolution between a BH and the host galaxy with multi-wavelength follow-up observations. The future high-resolution spectra will give more insight into the DLA and other absorption systems along the line of sight of J0306+1853.

Key words: galaxies: active – galaxies: high-redshift – quasars: absorption lines – quasars: emission lines – quasars: individual (SDSS J0306+1853)

1. INTRODUCTION

Supermassive black holes (SMBHs) reside in the centers of most galaxies, with masses in the range of $M_{\rm BH} \sim 10^6$–$10^9 M_{\odot}$. In the local universe, only a few objects have the measured black hole masses $M_{\rm BH} \sim 10^{10} M_{\odot}$ (e.g., McConnell et al. 2011; van den Bosch et al. 2012). Understanding when and how SMBHs form and grow is an important topic in extragalactic astronomy. One of the most direct ways to place constraints on the BH seeds and the growth of SMBHs is to study the masses of SMBHs hosted by luminous high-redshift quasars (e.g., Volonteri & Rees 2006; Trakhtenbrot et al. 2011).

BH masses in quasars can be estimated by the single-epoch virial mass estimate methods based on the low-ionization H β and Mg II emission lines (e.g., McLure & Dunlop 2004; Vestergaard & Peterson 2006). High-ionization lines such as C IV can also be used (e.g., Vestergaard & Peterson 2006); however, C IV is thought to be less reliable than H β and Mg II in limited signal-to-noise ratio (S/N) and resolution data (e.g., Shen et al. 2011; Trakhtenbrot & Netzer 2012; Denney et al. 2013).

The Sloan Digital Sky survey (SDSS; York et al. 2000) and the SDSS-III Baryonic Oscillation Spectroscopic Survey (Dawson et al. 2013) have provided the largest high-redshift quasar sample and resulted in the discovery of several hundred $z \gtrsim 4$ quasars with bolometric luminosity of several $10^{13}\,L_{\odot}$ (Schneider et al. 2010; Pâris et al. 2014). The SDSS quasar sample has been used to study the quasar luminosity function (QLF; Richards et al. 2006b; Ross et al. 2013) and BH mass function (BHMF; Kelly et al. 2010; Kelly & Shen 2013) at low and moderate redshifts. The BHMF suggested that the maximum mass of a black hole in a quasar to be $\sim 3 \times 10^{10} M_{\odot}$ (Kelly et al. 2010; Kelly & Shen 2013) at those redshifts. From the combination of SDSS quasars and the Stripe 82 faint quasar sample, McGreer et al. (2013) presented the most detailed study on the $z \sim 5$ QLF, especially at the faint end. However, the slope of the QLF at the bright end still has large uncertainties (e.g., Richards et al. 2006b; McGreer et al. 2013), mainly due to the small number of quasars observed to have extremely high luminosities (e.g., $M_{1450} \lesssim -27.5$).

The discoveries of luminous $z \sim 6$ quasars (e.g., Fan et al. 2001; Willott et al. 2010; Bañados et al. 2014) and $z \gtrsim 6.5$ quasars (e.g., Mortlock et al. 2011; Venemans et al. 2015) with a luminosity of $\sim 10^{13}\,L_{\odot}$ and Mg II based BH mass of $\sim 10^9\,M_{\odot}$ suggest that the fast growth of BHs may start from very early epochs ($z \gtrsim 20$) and involve massive seed BHs ($M_{\rm seed} \gtrsim 10^3 M_{\odot}$; e.g., Volonteri & Rees 2006). Recently, the first ten billion solar mass BHs at $z > 6$ have been discovered in an ultra-luminous quasar J0100+2802 at $z = 6.30$, selected from SDSS and *Wide-field Infrared Survey Explorer* (*WISE*; Wright et al. 2010) photometric data (Wu et al. 2015). This discovery posts a significant challenge to the theory of BH formation and the early BH–galaxy co-evolution again.

[9] Stromlo Fellow.

WISE mapped the whole sky at 3.4, 4.6, 12, and 22 μm (W1, W2, W3, and W4). Wu et al. (2012) suggested an efficient way to find high-redshift quasars by combining SDSS and *WISE* photometric data since most late-type stars have a significantly bluer *WISE* color than those of quasars. Carnall et al. (2015) used a similar method by combing optical and *WISE* colors to search $z \gtrsim 5.7$ quasars within the VST ATLAS survey. We are conducting a $z \gtrsim 5$ quasar survey based on SDSS–*WISE* colors and have discovered several ultra-luminous quasars (F. Wang et al. 2015, in preparation). Remarkably, we discovered an ultra-luminous quasar J0306+1853 at $z = 5.363$ with a bolometric luminosity of $L_{\rm bol} \sim 3.4 \times 10^{14} L_{\odot}$ and a BH mass of $1.07 \times 10^{10} M_{\odot}$. J0306+1853, along with J0100+2802, are the only two quasars yet known with $M_{1450} \sim -29$ and a BH mass up to ten billion solar masses at $z > 5$. Considering the high completeness of our selection method, these two quasars could be the only two ten billion solar mass BHs hosted by ultra-luminous quasars in the entire SDSS footprint. We also present the detection of a $z \sim 5$ metal-enriched damped Lyα system (DLA) in the spectrum of J0306+1853. Throughout this Letter, we use a Λ-dominated flat cosmology with $H_0 = 70$ km s^{-1} Mpc^{-1}, $\Omega_m = 0.3$, and $\Omega_\Lambda = 0.7$. The optical magnitudes in this Letter are in the AB system, and infrared magnitudes are in the Vega system.

2. OBSERVATIONS AND DATA

J0306+1853 was selected as a high-redshift quasar candidate based on SDSS and *WISE* photometric data (F. Wang et al. 2015, in preparation). J0306+1853 is undetected in the *u* and *g* bands but is relatively bright in the *r*, *i*, and *z* bands ($r = 19.89 \pm 0.03$, $i = 17.96 \pm 0.01$, $z = 17.49 \pm 0.02$) and is strongly detected in four *WISE* bands ($W1 = 14.31 \pm 0.03$, $W2 = 13.46 \pm 0.04$, $W3 = 10.51 \pm 0.10$, $W4 = 7.59 \pm 0.16$). With $r - i = 1.93$, $i - z = 0.47$, J0306+1853 is in the area of the *griz* color space strongly contaminated by M dwarfs (Richards et al. 2002). However, with $W1 - W2 = 0.86$, it is clearly separated from late-type stars. J0306+1853 can also be selected by the *z-W2/W1-W2* selection criteria used in Carnall et al. (2015). Besides, J0306+1853 is also detected in 2MASS (Skrutskie et al. 2006) in *J*, *H*, and *Ks* bands with $J = 16.50 \pm 0.13$, $H = 15.70 \pm 0.12$, and $Ks = 15.12 \pm 0.13$, respectively. The overall shape of the spectral energy distribution (SED) of J0306+1853 built from SDSS, 2MASS, and *WISE* photometry is consistent with the type I quasar composite SED (Richards et al. 2006a).

The first low-resolution optical spectrum of this source was obtained with the Lijiang 2.4 m telescope using the Yunnan Fainter Object Spectrograph and Camera (YFOSC) on 2013 November 25 (UT). A 22 minute exposure was taken with the G3 grism ($\lambda/\Delta\lambda \sim 680$ at 7000 Å) and a 1.″8 slit. This low-resolution spectrum clearly shows a sharp break at about 7700 Å and is consistent with a quasar at a redshift beyond 5.3. A possible $z \sim 5$ DLA system is also visible in the spectrum. To confirm this, a higher-resolution optical spectroscopic observation using *Magellan* Echellette spectrometer (MagE; Marshall et al. 2008) on the 6.5 m *Magellan*/Clay Telescope, with a 30 minute integration time, was taken on 2014 January 3. Our configuration of the MagE optical spectrum provides a resolution of $\lambda/\Delta\lambda = 4100$ in the wavelength range from 6000 to 10000 Å with a 1.″0 slit. The data were reduced by a custom-built pipeline (G. Becker 2015, private communication) and flux calibrated using a standard star.

In order to obtain the C IV and Mg II based BH masses and the metallicity of the DLA system in J0306+1853, we took a near-IR spectrum with the Folded-Port Infrared Echellette (FIRE; Schmidt et al. 2010), an IR echelle spectrograph on the 6.5 m *Magellan*/Baade Telescope. The observation was carried out on 2014 January 17 with an integration time of 60 minutes and provided a resolution of $R \sim 5000$ from 0.82 to 2.5 μm. We reduced the data using the IDL based pipeline (FIRE-HOSE; Simcoe et al. 2011), and the flux was calibrated with a nearby A0V telluric star. The magnitudes estimated from MagE and FIRE spectra are consistent with the SDSS and 2MASS photometric data ($\Delta m \lesssim 0.2$) and thus imply a small variability of J0306+1853 in a long time baseline. Finally, we combined the MagE optical spectrum and FIRE infrared spectrum and scaled it to match the SDSS *z*-band and 2MASS *J*-, *H*-, and *Ks*-band photometric data for absolute flux calibration (see Figure 1). The final spectrum yields a redshift of $z = 5.363 \pm 0.004$ based on the Mg II line fitting.

J0306+1853 is undetected in the NRAO VLA Sky Survey (Condon et al. 1998), the completeness limit of which is about 2.5 mJy at 1.4 GHz. This constrains the radio loudness of J0306+1853 to be $R = f_{6\,\rm cm}/f_{2500} \lesssim 76$, following Shen et al. (2011), where $f_{6\,\rm cm}$ and f_{2500} are the flux density (f_ν) at rest-frame 6 cm and 2500 Å, respectively. The radio loudness upper limit, together with the small variability, suggests that J0306+1853 is not a beamed source.

3. LUMINOSITY AND BLACK HOLE MASS MEASUREMENTS

To derive line widths and continuum luminosities used for single-epoch virial BH mass estimators, we performed a least χ^2 global fitting to the combined optical and near-IR spectrum. The spectrum was de-reddened for Galactic extinction using the Cardelli et al. (1989) Milky Way reddening law and $E(B-V)$ derived from the Schlegel et al. (1998) dust map. The spectrum was then shifted to rest frame using the redshift based on Mg II. We first fit a pseudo-continuum model to account for the power-law continuum, Fe II emission, and Balmer continuum in the line free region. Templates of Fe II emission were from Shen et al. (2011) by combining the Vestergaard & Wilkes (2001) template (1000–2200 Å) and the Salviander et al. (2007) template (2200–3090 Å). The Fe II template is broadened by convolving the template with Gaussians with a range of intrinsic line widths and then scaled to match the observed spectrum. We model the Balmer continuum following De Rosa et al. (2011), which assumed a partially optically thick gas cloud with a uniform temperature $T_e = 15{,}000$ K and normalized to the power-law continuum at $\lambda_{\rm rest} = 3675$ Å. From the best pseudo-continuum fit, we measured the rest-frame 3000 and 1350 Å power-law luminosities as 2.04×10^{47} and 3.46×10^{47} ergs s^{-1}, and the absolute magnitude at rest-frame 1450 Å as $M_{1450,AB} = -28.92 \pm 0.04$. By assuming an empirical conversion factor from the luminosity at 1350 Å (Shen et al. 2011), we estimate the bolometric luminosity as $L_{\rm bol} = 3.81 \times L_{1350\,\text{Å}} = (1.32 \pm 0.08) \times 10^{48}$ erg s^{-1}. We get the Eddington mass to be $\sim 10^{10} M_{\odot}$ by assuming Eddington accretion, which is an approximate lower limit of the BH mass (e.g., Kurk et al. 2007).

We then fit individual emission lines after subtracting the pseudo-continuum. As the two-Gaussian model provided a sufficiently good model of the line profiles of Mg II and

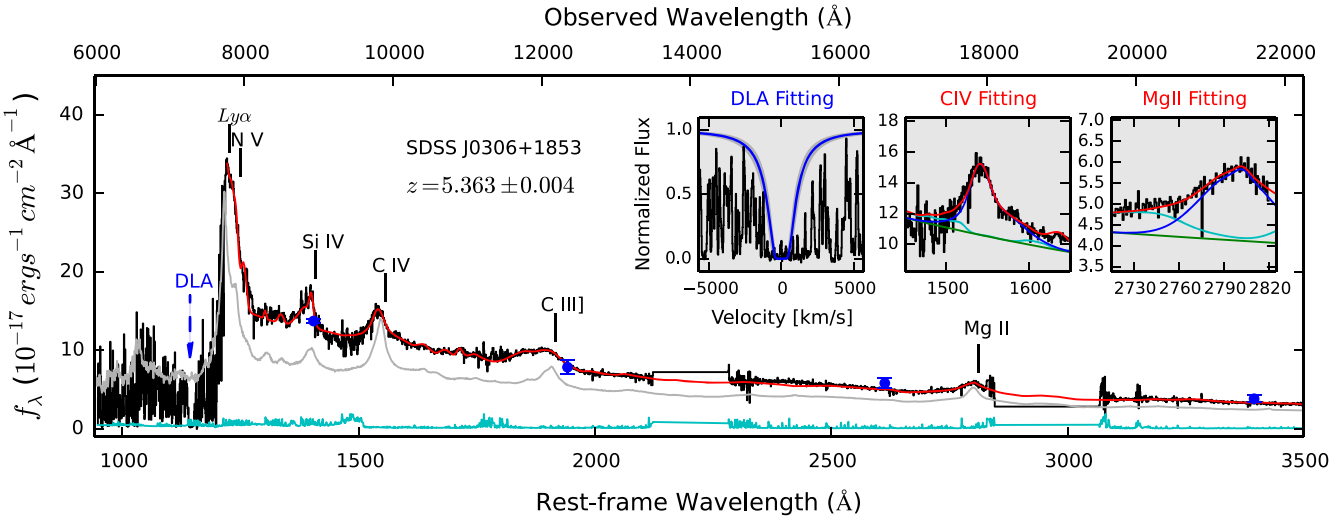

Figure 1. Spectrum of J0306+1853. The red line shows the best fitting and the gray line shows the SDSS composite spectrum (Vanden Berk et al. 2001). The cyan line shows the noise spectrum. The blue points, from left to right, represent SDSS *z*-band, 2MASS *J*, *H*, and *Ks* photometry. The blue arrow labels the position of a DLA at $z = 4.986$. The left inner plot shows the Voigt profile fitting of the DLA. The blue curve is the best fit and the gray shading includes the 95% limit. The column density of the DLA is $N_{\rm HI} = 10^{20.50^{+0.10}_{-0.12}}$ cm^{-2}. Two right-hand small insets show the fitting of C IV and Mg II emission lines; the green lines represent a power-law and Balmer continuum, the cyan lines denote Fe II contribution, and the blue lines are contributions from C IV and Mg II emissions. The gaps in the spectrum are due to the low sky transparency there.

C IV given the S/N of our spectra, we use two Gaussians to fit Mg II and C IV emission lines, respectively. For other emission lines, we use one Gaussian to fit isolated lines and multiple Gaussians to fit blended lines, the same as was done in Jiang et al. (2007). The best fitting is shown in Figure 1. We noticed that a portion of the red part of the Mg II profile is missed in the FIRE spectrum due to the low transmission, which may cause some uncertainties in the estimation of Mg II line width. The FWHMs and equivalent widths (EWs) of Mg II and C IV are 5722 ± 640 km s^{-1}, 22.6 ± 2.8 Å and 7320 ± 680 km s^{-1}, 25.1 ± 2.1 Å, respectively.

To estimate the black hole mass of J0306+1853, we adopt the relation obtained by Vestergaard & Osmer (2009) for Mg II estimator:

$$\frac{M_{\rm BH}({\rm Mg\ II})}{M_\odot} = 10^{6.86}\left[\frac{\lambda L_\lambda(3000\ {\rm Å})}{10^{44}\ {\rm erg\ s^{-1}}}\right]^{0.5}\left[\frac{{\rm FWHM(Mg\ II)}}{10^3\ {\rm km\ s^{-1}}}\right]^2 \quad (1)$$

and Vestergaard & Peterson (2006) for C IV estimator:

$$\frac{M_{\rm BH}({\rm C\ IV})}{M_\odot} = 10^{6.66}\left[\frac{\lambda L_\lambda(1350\ {\rm Å})}{10^{44}\ {\rm erg\ s^{-1}}}\right]^{0.53}\left[\frac{{\rm FWHM(C\ IV)}}{10^3\ {\rm km\ s^{-1}}}\right]^2. \quad (2)$$

These relations give the black hole mass of J0306+1853 as $M_{\rm BH}({\rm Mg\ II}) = (1.07 \pm 0.27) \times 10^{10}\ M_\odot$ and $M_{\rm BH}({\rm C\ IV}) = (2.16 \pm 0.48) \times 10^{10}\ M_\odot$. The Eddington ratio is $L_{\rm bol}/L_{\rm Edd} = 0.95$ for the Mg II based measurement and 0.47 for the C IV based measurement. The uncertainties of the BH mass are measured from the 68% range of the distributions from fitting 200 mock spectra generated using the method in Shen et al. (2011). Note that it does not include systematic errors of using different BH mass estimators. By using different Fe II templates (e.g., Tsuzuki et al. 2006; Salviander et al. 2007) and different estimators (e.g., McLure & Dunlop 2004; Vestergaard & Osmer 2009; Wang et al. 2009; Shen et al. 2011; Trakhtenbrot & Netzer 2012), the Mg II based BH mass of J0306+1853 could be in the range of 7.3–20.7 billion solar mass and the systematic uncertainties of Mg II based BH masses could be ~0.5 dex (e.g., Shen 2013). However, the Mg II based BH mass measurement is still the most reliable method for measuring BH masses at high redshift. We will only use the Mg II based BH mass for subsequent discussion. Figure 2 shows the distribution of quasar bolometric luminosities and black hole masses estimated from the Mg II lines for a large sample of quasars from literature over a wide range of redshifts. Adopting the $M_{\rm BH}$ estimate based on McLure & Dunlop (2004) calibration, the BH in J0306+1853 is more massive by ~0.25 dex than the most massive one found in Trakhtenbrot et al. (2011), or by 0.38 dex compared with the De Rosa et al. (2011) study. It is close to the most massive black holes at any redshift, and together with J0100+2822 (Wu et al. 2015), the most massive BH yet discovered at $z > 5$. Considering the high completeness of our selection method, J0306+1853 and J0100+2802 could be the only two ten billion solar mass BHs hosted by ultra-luminous quasars at $z > 5$ in the SDSS footprint.

4. A DLA SYSTEM AT $z \sim 5.0$

DLAs are atomic hydrogen gas clouds measured in absorptions to background quasars with a column density higher than 2×10^{20} cm^{-2}, which are unique laboratories for understanding the conversion of neutral gas into stars at high redshift (Wolfe et al. 2005). However, the number of known high-redshift DLAs is very rare and only about 10 DLAs have been discovered at $z > 4.7$ (Rafelski et al. 2012). The studies of metallicities of these high-redshift DLAs suggest a rapid decline in metallicity of DLAs at $z \sim 5$ (Rafelski et al. 2012, 2014).

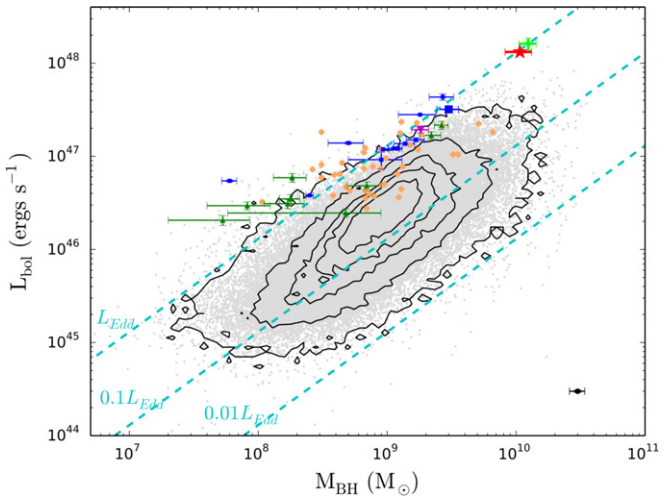

Figure 2. Distribution of quasar bolometric luminosities and black hole masses estimated from Mg II lines. The red star represents J0306+1853, and the light green cycle represents the luminous quasar J0100+2802 at $z = 6.30$ (Wu et al. 2015). The brown points denote $z \sim 4.8$ quasars from Trakhtenbrot et al. (2011). The blue squares denote SDSS high-redshift quasars at $z \sim 6$ (Jiang et al. 2007; Kurk et al. 2007; De Rosa et al. 2011). The green triangles denote CFHQS high-redshift quasars at $z \sim 6$ (Willott et al. 2010; De Rosa et al. 2011). The purple inverted triangle denotes the most distance quasar ULAS J1120+0641 at $z = 7.085$ (Mortlock et al. 2011). Black contours and gray dots denote SDSS low-redshift quasars from Shen et al. (2011; with broad absorption line quasars excluded). The error bars represent the 1σ standard measurement errors, and the mean error bar for low-redshift quasars is presented in the bottom right corner. The dashed lines denote the luminosity in different fractions of Eddington luminosity. Note that the systematic uncertainties (not included in error bars) of virial BH masses could be up to a factor of 0.5 dex.

A $z = 4.986$ DLA system is clearly present in the absorption spectrum of J0306+1853 (Figure 1). We determine the $N_{\rm HI}$ value of the DLA system by fitting a Voigt profile using the method of Rafelski et al. (2012). The best fit yields a column density of $N_{\rm HI} = 10^{20.50^{+0.10}_{-0.12}}$ cm^{-2}. We estimate the error on the $N_{\rm HI}$ value by manually selecting values that ensure that $N_{\rm HI}$ solutions when assuming a single component of DLA plus a possible deblending of Lyα forest in the wings. However, we need to caution that the systematic effects of line saturation and continuum placement will lend larger uncertainties in most cases (e.g., Rafelski et al. 2012), and the systematic uncertainties for all the measurements could be ~0.1 dex.

This DLA is also associated with a number of corresponding metal lines, including C II λ1334, Si II λ1304, λ1526, O I λ1302, C IV λ1548, λ1550, and Mg II λ2796, λ2803 (Figure 3). Rafelski et al. (2012) suggest that S and Si are ideal elements for determining metallicity. We use the apparent optical depth method (Savage & Sembach 1991) to derive the total column density of Si with Si II λ1304, λ1526 absorption lines and find $N_{\rm Si} = 10^{14.8}$ cm^{-2}. The rest-frame EW of Si II λ1304 and Si II λ1526 are 0.070 ± 0.005 Å and 0.10 ± 0.007 Å, respectively. We estimate that the metallicity of this DLA is [M/H] $= -1.3 \pm 0.1$. Note that the error does not include systematic uncertainties. This makes it one of the most metal-rich DLAs found to date at $z \gtrsim 5$. Although the metallicity of the DLA in J0306+1853 is about 0.7 dex higher than the average metallicity of other $z \sim 5$ DLAs, the existence of such a system is still consistent with the rapid decline in metallicity of DLAs at $z \gtrsim 5$ (Rafelski et al. 2014).

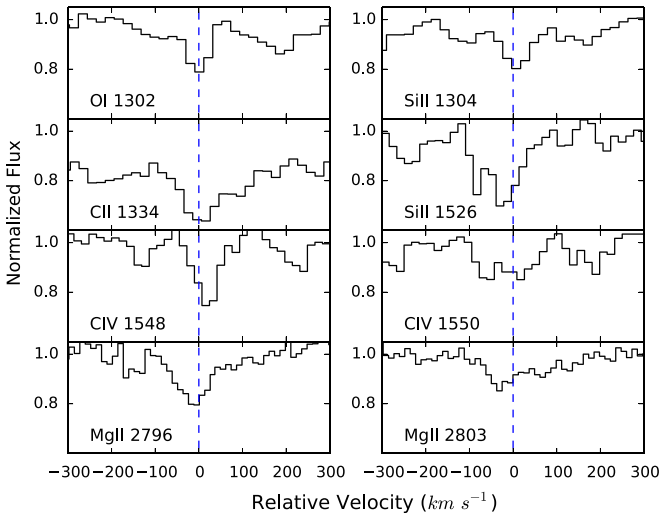

Figure 3. Velocity profiles of metal transitions for the $z = 4.986$ DLA. The total column density of Si is $N_{\rm Si} = 10^{14.8}$ cm^{-2}, and the metallicity of this DLA is [M/H] $= -1.3 \pm 0.1$. See Section 4 for details.

5. DISCUSSION AND SUMMARY

Although gravitational lensing is a possible explanation for its high luminosity and inferred BH mass, we do not expect a large lensing magnification, as J0306+1853 is an unresolved object in the FIRE acquisition image under the 1.″0 seeing condition. Besides, J0306+1853 could not possibly be a beamed source as implied by the small flux variability, small radio loudness, and normal broad emission lines. The bright-end slope of the $z \sim 5$ QLF is measured to be $\beta \lesssim -4$, indicating a rapid decline in the space density of luminous quasars at high redshift (McGreer et al. 2013). We searched the entire SDSS footprint (~14,000 deg^2) with our SDSS–*WISE* selection method and found J0306+1853 to be the only quasar with such a high luminosity at this redshift. Since our selection method is highly complete for luminous quasars at $z \gtrsim 5$ (J. Yang et al. 2015, in preparation), J0306+1853 is possibly the only quasar with $M_{1450} < -28.9$ at redshift $z \gtrsim 5$ in the SDSS footprint. From the prediction using the $z \sim 5$ QLF (McGreer et al. 2013), the number of quasars with such high luminosity at $4.7 \lesssim z \lesssim 5.4$ is about two in the whole sky and the probability of finding one such luminous quasar in the SDSS footprint with our selection method is ~35%. Together with J0100+2802 at higher redshift, J0306+1853 is the only other known quasar with M_{1450} up to ~ -29 at $z > 5$. Although the discovery of J0306+1853 is consistent with the expectation from the current measurements of the QLF, its existence (and our finding of only a single object at this luminosity) shows that the luminosity function extends to much greater luminosities than previously explored and sets a strong constraint on the bright-end slope. A detailed study of the QLF will be presented in a forthcoming paper (J. Yang et al. 2015, in preparation) based on a complete sample of SDSS–*WISE* selected $z \sim 5$ quasars.

Kelly & Shen (2013) estimated the BHMF and Eddington ratio functions at $z \lesssim 5$ for Type 1 quasars from ~58,000 uniformly selected SDSS quasars. Assuming there is no evolution from redshift of 4.75–5.25, their BHMF predicts that there should be several tens of quasars with a BH mass larger than 10 billion $M_\odot$ at a redshift between 5.0 and 5.5. Since J0306+1853 is the only quasar discovered in our survey

with an $M_{\rm BH}$ of $10^{10}\,M_{\odot}$ and an Eddington ratio close to the order of unity discovered, this would imply that there is a population of fainter quasars with a lower Eddington ratio hosting $10^{10}\,M_{\odot}$ black holes. A complete survey of such objects requires high-quality near-IR spectroscopy of a large sample of fainter $z \sim 5$ quasars.

Absorption spectra of high-redshift quasars provide one of the most powerful tools for studying the intergalactic medium (IGM) in the early universe (e.g., Simcoe et al. 2011). Future high signal-to-noise, high-resolution spectra of ultra-luminous quasars such as J0306+1853 will be very promising probes for the study of the IGM evolution and the shape of the ionizing background at $z \gtrsim 5$.

We thank the referee for providing constructive comments and suggestions. F. W. and X.-B. W. are grateful for the support of NSFC grant No.11373008, the Strategic Priority Research Program "The Emergence of Cosmological Structures" of the Chinese Academy of Sciences, grant No. XDB09000000, and the National Key Basic Research Program of China 2014CB845700. X.F. and I. D. M. are thankful for support from US NSF grant AST 11-07682. Funding for the Lijiang 2.4 m telescope is provided by the Chinese Academy of Sciences and the People's Government of Yunnan Province. This Letter includes data gathered with the 6.5 m *Magellan* Telescopes located at Las Campanas Observatory, Chile. We thank George Becker for providing MagE spectral data reduction. This research uses data obtained through the Telescope Access Program (TAP), which has been funded by the Strategic Priority Research Program "The Emergence of Cosmological Structures" (grant No. XDB09000000), National Astronomical Observatories, Chinese Academy of Sciences, and the Special Fund for Astronomy from the Ministry of Finance. We acknowledge the use of SDSS, 2MASS, and *WISE* photometric data.

Facilities: 2.4 m/YNAO (YFOSC), *Magellan*: Clay (MagE), *Magellan*: Baade (FIRE), Sloan (SDSS), *WISE*, 2MASS.

REFERENCES

Bañados, E., Venemans, B. P., Morganson, E., et al. 2014, AJ, 148, 14
Cardelli, J. A., Clayton, G. C., & Mathis, J. S. 1989, ApJ, 345, 245
Carnall, A. C., Shanks, T., Chehade, B., et al. 2015, MNRAS, 451, L16
Condon, J. J., Cotton, W. D., Greisen, E. W., et al. 1998, AJ, 115, 1693
Dawson, K. S., Schlegel, D. J., Ahn, C. P., et al. 2013, AJ, 145, 10
Denney, K. D., Pogge, R. W., Assef, R. J., et al. 2013, ApJ, 775, 60
de Rosa, G., Decarli, R., Walter, F., et al. 2011, ApJ, 739, 56
Fan, X., Strauss, M., Richards, G., et al. 2001, AJ, 121, 31
Jiang, L., Fan, X., Vestergaard, M., et al. 2007, AJ, 134, 1150
Kelly, B. C., & Shen, Y. 2013, ApJ, 764, 45
Kelly, B. C., Vestergaard, M., Fan, X., et al. 2010, ApJ, 719, 1315
Kurk, J. D., Walter, F., Fan, X., et al. 2007, ApJ, 669, 32
Marshall, J. L., Burles, S., Thompson, I. B., et al. 2008, Proc. SPIE, 7014, 169
McConnell, N. J., Ma, C.-P., Gebhardt, K., et al. 2011, Natur, 480, 215
McGreer, I. D., Jiang, L., Fan, X., et al. 2013, ApJ, 768, 105
McLure, R. J., & Dunlop, J. S. 2004, MNRAS, 352, 1390
Mortlock, D. J., Warren, S. J., Venemans, B. P., et al. 2011, Natur, 474, 616
Pâris, I., Petitjean, P., Aubourg, Ê, et al. 2014, A&A, 563, A54
Rafelski, M., Neeleman, M., Fumagalli, M., et al. 2014, ApJL, 782, L29
Rafelski, M., Wolfe, A. M., Prochaska, J. X., et al. 2012, ApJ, 755, 89
Richards, G. T., Fan, X., Newberg, H. J., et al. 2002, AJ, 123, 2945
Richards, G. T., Lacy, M., Storrie-Lombardi, L. J., et al. 2006a, AJ, 166, 470
Richards, G. T., Strauss, M. A., Fan, X., et al. 2006b, AJ, 131, 2766
Ross, N. P., McGreer, I. D., White, M., et al. 2013, ApJ, 773, 14
Salviander, S., Shields, G. A., Gebhardt, K., et al. 2007, ApJ, 662, 131
Savage, B. D., Sembach, K. R., et al. 1991, ApJ, 379, 245
Schlegel, D. J., Finkbeiner, D. P., & Davis, M. 1998, ApJ, 500, 525
Schmidt, L. M., Jurgenson, C. A., Santoro, F. G., & Teare, S. W. 2010, Proc. SPIE, 7735, 773538
Schneider, D. P., Richards, G. T., Hall, P. B., et al. 2010, AJ, 139, 2360
Shen, Y. 2013, BASI, 41, 61
Shen, Y., Richards, G. T., Strauss, M. A., et al. 2011, ApJS, 194, 45
Simcoe, R. A., Cooksey, K. L., Matejek, K., et al. 2011, ApJ, 743, 21
Skrutskie, M. F., Cutri, R. M., Stiening, R., et al. 2006, AJ, 131, 1163
Trakhtenbrot, B., & Netzer, H. 2012, MNRAS, 427, 3081
Trakhtenbrot, B., Netzer, H., Lira, P., et al. 2011, ApJ, 730, 7
Tsuzuki, Y., Kawara, K., Yoshii, Y., et al. 2006, ApJ, 650, 57
van den Bosch, R. C. E., Gebhardt, K., Gültekin, K., et al. 2012, Natur, 491, 729
Vanden Berk, D. E., Richards, G. T., Bauer, A., et al. 2001, AJ, 122, 549
Venemans, B. P., Bañados, E., Decarli, R., et al. 2015, ApJL, 801, L11
Vestergaard, M., & Osmer, P. S. 2009, ApJ, 699, 800
Vestergaard, M., & Peterson, B. M. 2006, ApJ, 641, 689
Vestergaard, M., & Wilkes, B. J. 2001, ApJS, 134, 1
Volonteri, M., & Rees, M. 2006, ApJ, 650, 669
Wang, J.-G., Dong, X.-B., Wang, T.-G., et al. 2009, ApJ, 707, 1334
Willott, C. J., Albert, L., Arzoumanian, D., et al. 2010, AJ, 140, 546
Wolfe, A. M., Gawiser, E., & Prochaska, J. X. 2005, ARA&A, 43, 861
Wright, E. L., Eisenhardt, P., Mainzer, A. K., et al. 2010, AJ, 140, 1868
Wu, X.-B., Hao, G., Jia, Z., et al. 2012, AJ, 144, 49
Wu, X.-B., Wang, F., Fan, X., et al. 2015, Natur, 518, 512
York, D. G., Adelman, J., Anderson, J. E., Jr., et al. 2000, AJ, 120, 1579